Extension and Validation of an Advanced Integral Equation Model for Bistatic Scattering from Rough Surfaces

Kuan-Liang Chen[1], Kun-Shan Chen[2, 3, *], Zhao-Liang Li[3], and Yu Liu[2]

Abstract—This paper deals with the modeling of bistatic scattering from a randomly rough surface. An advanced integral equation model is presented by giving its general framework of model developments, model expressions, and predictions of bistatic scattering for various surface parameters. Extension work to improve the model accuracy is also reported in more detail. In particular, the transition function for the Fresnel reflection coefficient is in more general form. Model predictions are illustrated, demonstrated, and validated by extensive comparisons with numerical simulations. The updated advanced integral equation model remains a compact algebraic form for single scattering and substantially improves prediction accuracy in bistatic scattering that is drawing more emerging applications in earth remote sensing.

1. INTRODUCTION

Electromagnetic wave scattering from a randomly rough surface is of palpable importance in many fields of disciplines and bears itself in various applications spanning from surface treatment to remote sensing of terrain and sea [1–6]. For example, it has been a common practice to retrieve, by analyzing the sensitivity of the scattering behavior and mechanisms, the geophysical parameters of interest from the scattering and/or emission measurements. Another example is that by knowing the backscattering patterns, one may be able to detect the presence of the undesired random roughness of a reflective surface such as antenna reflector, and thus accordingly devise a means to correct or compensate the phase errors. Therefore, researchers have been both theoretically and practically motivated to study the electromagnetic wave scattering from the random surfaces. Research and progress of this topic has been documented well and is still kept updated.

In order to tackle the complex and sometimes intricate mathematical derivations and yet to retain a high level of accuracy beyond conventional models, notably, Kirchhoff and small perturbation method (SPM), the integral equation model (IEM) has been developed by Fung et al. [3, 7, 8] under several physical-justified assumptions. Among the assumptions, one was to use a simplified Green's function by dropping off the phase term associated with the random surface height. Doing so might be more profoundly critical among all assumptions but greatly alleviating the burden of mathematical derivations, and yet unavoidably degrading the model accuracy, to certain extents, depending upon the surface property and observation geometry. Nevertheless, the IEM model proves to perform very well in backscattering and offers to seamlessly bridge the gap between the Kirchhoff and SPM models.

Driven by the need of predicting bistatic scattering and microwave emissivity, much effort has been devoted to further improving the IEM accuracy [9–19] by removing some of the assumptions originally

imposed for the purpose of mathematical simplicity during the course of derivation. Another leap forward step was the introduction of a transition function into the Fresnel reflection coefficients to take spatial dependence into account, removing the restrictions on the limits of surface roughness and permittivity [3, 11]. Though the approach is of heuristic but self-consistent, it proves to work well for a broad range of surface dielectric and geometric parameters [6, 11, 14].

As will be presented in later sections, the propagation vectors in upward and downward directions are graphically decomposed to better gain physical insights into the second order scattering mechanism. This decomposition allows us to mathematically express all the necessary terms to account for the scattering components. We generalize the transition function of Fresnel reflection to bistatic scattering plane. The location of the dips in scattering plane is accurately predicated, and the scattering pattern has been studied more extensively. Comparisons with experimental measurements have been limited due to very limited well-controlled measured data available in the literature. Numerical simulation is an alternative to cross-verify the scattering behavior and is under working. Another issue is the complete multiple scattering terms needed to be included when the surface slope becomes sufficiently large.

2. THE ADVANCED INTEGRAL EQUATION MODEL

2.1. Formulation of the Wave Scattering from a Rough Surface

Referring to Figure 1, consider that a plane wave impinges onto a dielectric rough surface which scatters waves up into the incident plane and down into the lower medium, with the electric and magnetic fields written as

$$\vec{E}^i = \hat{p} E_0 \exp\left[-j\left(\vec{k}_i \cdot \vec{r}\right)\right], \tag{1}$$

$$\vec{H}^i = \frac{1}{\eta} \hat{k}_i \times \vec{E}^i; \tag{2}$$

where $j = \sqrt{-1}$; i denotes incident wave, $\hat{p}$ the unit polarization vector, E_0 the amplitude of the incident electric field, and η the intrinsic impedance of the upper medium, respectively. The position and wavenumber vectors in incident and scattering directions are defined as follows, respectively

$$\vec{r} = x\hat{x} + y\hat{y} + z\hat{z}$$

$$\vec{k}_i = k\hat{k}_i = \hat{x}k_{ix} + \hat{y}k_{iy} + \hat{z}k_{iz}; \quad k_{ix} = k\sin\theta_i\cos\phi_i, \quad k_{iy} = k\sin\theta_i\sin\phi_i, \quad k_{iz} = k\cos\theta_i$$

$$\vec{k}_s = k\hat{k}_s = \hat{x}k_{sx} + \hat{y}k_{sy} + \hat{z}k_{sz}; \quad k_{sx} = k\sin\theta_s\cos\phi_s, \quad k_{sy} = k\sin\theta_s\sin\phi_s, \quad k_{sz} = k\cos\theta_s$$

For linearly horizontal-polarized and vertical-polarized waves, the polarization vector $\hat{p}$, for incident and scattering waves, is defined as

$$\hat{h}_i = -\hat{x}\sin\phi_i + \hat{y}\cos\phi_i$$
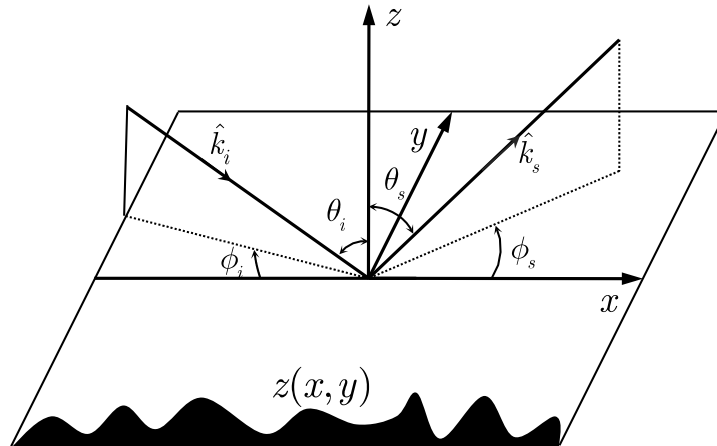
Figure 1. Wave scattering geometry.

$$\hat{v}_i = \hat{h}_i \times \hat{k}_i = -\left(\hat{x}\cos\theta_i\cos\phi_i + \hat{y}\cos\theta_i\sin\phi_i + \hat{z}\sin\theta_i\right)$$
$$\hat{h}_s = \hat{\phi} = -\hat{x}\sin\phi_s + \hat{y}\cos\phi_s$$
$$\hat{v}_s = \hat{\theta} = \hat{h}_s \times \hat{k}_s = \hat{x}\cos\theta_s\cos\phi_s + \hat{y}\cos\theta_s\sin\phi_s - \hat{z}\sin\theta_s$$

The scattered fields according to the Stratton-Chu formula may be expressed as [2, 5]

$$\vec{E}_s(\vec{r}) = \oiint_{S'} dS' \left\{ i\omega\mu \left[\hat{n} \times \vec{H}\left(\vec{r}'\right)\right] G\left(\vec{r},\vec{r}'\right) + \left[\hat{n}\cdot\vec{E}\left(r'\right)\right]\nabla' G\left(\vec{r},\vec{r}'\right) + \left[\hat{n}\times\vec{E}\left(r'\right)\right]\times\nabla' G\left(\vec{r},\vec{r}'\right) \right\} \quad (3a)$$

$$\vec{H}_s(\vec{r}) = \oiint_{S'} dS' \left\{ -i\omega\varepsilon \left[\hat{n} \times \vec{E}\left(\vec{r}'\right)\right] G\left(\vec{r},\vec{r}'\right) + \left[\hat{n}\cdot\vec{H}\left(r'\right)\right]\nabla' G\left(\vec{r},\vec{r}'\right) + \left[\hat{n}\times\vec{H}\left(r'\right)\right]\times\nabla' G\left(\vec{r},\vec{r}'\right) \right\} \quad (3b)$$

where G is the Green's function, $\hat{n}$ the unit normal vector pointing to the scattering region, and the integration is performed over the rough surface S'. The total field is sum of the incident field, which is known, and the scattered field, which is unknown, is to be determined. For a source free region as in our case, mathematically, it is expressed as [20]

$$\vec{E}(\vec{r}) = \Upsilon\vec{E}_i(\vec{r}) - \frac{\Upsilon}{4\pi}\oiint dS' \left\{ i\omega\mu\left[\hat{n}\times\vec{H}\right]G - \left[\hat{n}\times\vec{E}\right]\times\nabla' G - \left[\hat{n}\cdot\vec{E}\right]\nabla' G \right\} \quad (4a)$$

$$\vec{H}(\vec{r}) = \Upsilon\vec{H}_i(\vec{r}) + \frac{\Upsilon}{4\pi}\oiint dS' \left\{ i\omega\varepsilon\left[\hat{n}\times\vec{E}\right]G + \left[\hat{n}\times\vec{H}\right]\times\nabla' G + \left[\hat{n}\cdot\vec{H}\right]\nabla' G \right\} \quad (4b)$$

where $\Upsilon = (1 - \Omega/4\pi)^{-1}$, $\Omega = \begin{cases} 0, & \vec{r} \notin S' \\ 2\pi, & \vec{r} \in S' \end{cases}$.

To solve the above integral equations, we follow the approach in [3, 7]. Once the surface fields $\hat{n}\times\vec{E}$, $\hat{n}\times\vec{H}$ are solved, the scattered filed are obtained by (3a) and (3b). Note that the normal components of the surface fields are related to tangential components by surface divergence operation. The scattering coefficient with q polarization is then calculated as [2]:

$$\sigma_{qp}^o = \frac{4\pi R^2 \mathscr{R}e\left\{\left\langle\left|E_{qp}^s\right|^2\right\rangle\right\}}{A_0\cos\theta_i\mathscr{R}e\left\{|E_i|^2\right\}} \quad (5)$$

where R is the range from surface to observation point, and A_0 is illuminated overlapping area, confined by transmitting and receiving antenna beam patterns, over the surface.

2.2. Surface Tangential Fields

Equation (3) states the Huygens' Principle [5], and the field solution in a given volume V' is completely determined by the tangential fields specified over the surface S' enclosing V'. To find the surface fields, one has to solve the pair of Fredholm integral equations of 2nd kind. For rough surface with irregular boundary, completely analytic solution is almost prohibitive. Instead, we seek an approximate estimate of the surface tangential fields by taking vector product with the unit surface normal on both sides of Equations (4a), (4b) and, after some reformulations [21], by using the iterative scheme to find the estimates.

In IEM modelling [3, 7], the estimation of surface fields is the sum of the Kirchhoff field and the complementary field,

$$\left(\hat{n}\times\vec{E}_p\right) = \left(\hat{n}\times\vec{E}_p\right)_k + \left(\hat{n}\times\vec{E}_p\right)_c \quad (6a)$$

$$\left(\hat{n}\times H_p\right) = \left(\hat{n}\times\vec{H}_p\right)_k + \left(\hat{n}\times\vec{H}_p\right)_c \quad (6b)$$

where the Kirchhoff fields can be expressed as

$$\left(\hat{n}\times\vec{E}_p\right)_k = \hat{n}\times\left[(1-R_v)\hat{p} + (R_v+R_h)\left(\hat{p}\cdot\hat{t}\right)\hat{t}\right]E^i, \quad (7a)$$

$$\eta_1\left(\hat{n}\times\vec{H}_p\right)_k = \hat{n}\times\hat{k}_i\times\left[(1+R_v)\hat{p} + (R_v+R_h)\left(\hat{p}\cdot\hat{t}\right)\hat{t}\right]E^i. \quad (7b)$$

The complementary surface fields, which corrects the Kirchhoff estimates, are written as

$$\left(\hat{n} \times \vec{E}_v\right)_c = -\frac{1}{4\pi}\left[\hat{n} \times \int \left(1 - R_v\right)\vec{\mathcal{E}}_v ds' + \hat{n} \times \int \left(1 + R_v\right)\vec{\mathcal{E}}_{vt} ds'\right.$$
$$\left. - \left(R_v + R_h\right)\left(\hat{n} \times \hat{t}\right)\left(\hat{n} \times \hat{t}\right) \cdot \hat{n} \times \int \left(\vec{\mathcal{E}}_v - \vec{\mathcal{E}}_{vt}\right)ds'\right] \tag{8a}$$

$$\left(\hat{n} \times \vec{E}_h\right)_c = -\frac{1}{4\pi}\left[\hat{n} \times \int \left(1 + R_h\right)\vec{\mathcal{E}}_h ds' + \hat{n} \times \int \left(1 - R_h\right)\vec{\mathcal{E}}_{ht} ds'\right.$$
$$\left. + \left(R_v + R_h\right)\hat{t}\hat{t} \cdot \hat{n} \times \int \left(\vec{\mathcal{E}}_h - \vec{\mathcal{E}}_{ht}\right)ds'\right] \tag{8b}$$

$$\left(\hat{n} \times \vec{H}_v\right)_c = \frac{1}{4\pi}\left[\hat{n} \times \int \left(1 + R_v\right)\vec{\mathcal{H}}_v ds' + \hat{n} \times \int \left(1 - R_v\right)\vec{\mathcal{H}}_{vt} ds'\right.$$
$$\left. - \left(R_v + R_h\right)\hat{t}\hat{t} \cdot \hat{n} \times \int \left(\vec{\mathcal{H}}_v - \vec{\mathcal{H}}_{vt}\right)ds'\right] \tag{9a}$$

$$\left(\hat{n} \times \vec{H}_h\right)_c = \frac{1}{4\pi}\left[\hat{n} \times \int \left(1 - R_h\right)\vec{\mathcal{H}}_h ds' + \hat{n} \times \int \left(1 + R_h\right)\vec{\mathcal{H}}_{ht} ds'\right.$$
$$\left. + \left(R_v + R_h\right)\left(\hat{n} \times \hat{t}\right)\left(\hat{n} \times \hat{t}\right) \cdot \hat{n} \times \int \left(\vec{\mathcal{H}}_h - \vec{\mathcal{H}}_{ht}\right)ds'\right] \tag{9b}$$

In the above expressions, we make use of a local coordinate defined by $[\hat{k}_i, \hat{t}, \hat{d}]$ in Figure 2 [2, 3]. The unknown electric and magnetic fields that appear inside the integrals above are expressed as

$$\vec{\mathcal{E}}_p = jk\eta\left(\hat{n} \times \vec{H}_p\right)G - \left(\hat{n} \times \vec{E}_p\right) \times \nabla'G - \left(\hat{n} \cdot \vec{E}_p\right)\nabla'G \tag{10a}$$

$$\vec{\mathcal{H}}_p = j\frac{k}{\eta}\left(\hat{n} \times \vec{E}_p\right)G - \left(\hat{n} \times \vec{H}_p\right) \times \nabla'G - \left(\hat{n} \cdot \vec{H}_p\right)\nabla'G \tag{10b}$$

$$\vec{\mathcal{E}}_{pt} = -\left[jk_t\eta_t\left(\hat{n} \times \vec{H}_p\right)G_t - \left(\hat{n} \times \vec{E}_p\right) \times \nabla'G_t - \frac{1}{\varepsilon_r}\left(\hat{n} \cdot \vec{E}_p\right)\nabla'G_t\right] \tag{11a}$$

$$\vec{\mathcal{H}}_{pt} = -\left[j\frac{k_t}{\eta_t}\left(\hat{n} \times \vec{E}_p\right)G_t - \left(\hat{n} \times \vec{H}_p\right) \times \nabla'G_t - \frac{1}{\mu_r}\left(\hat{n} \cdot \vec{H}_p\right)\nabla'G_t\right] \tag{11b}$$

where η_t is the intrinsic impedance of the lower medium, the wave transmitted region. (10) and (11) involve Green's functions and theirs gradients in the upper and lower media. To seek solutions by
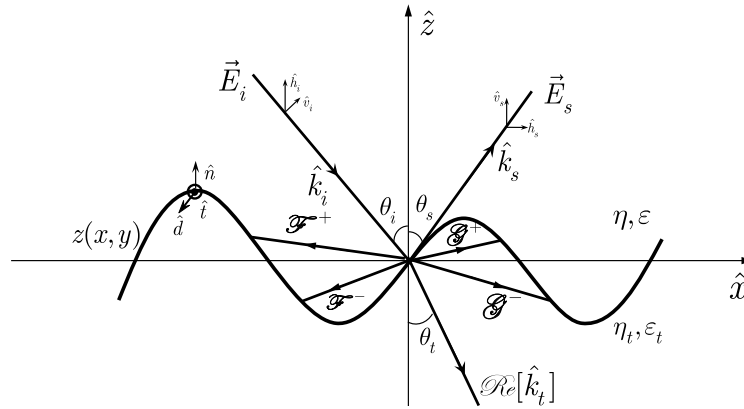
Figure 2. Geometry of scattering from a rough surface, where $\mathscr{F}^{\pm}$, $\mathscr{G}^{\pm}$ respectively represent the upward re-radiation and downward re-radiation, going through upper medium and lower medium.

iterative scheme we make use of the spectral form, instead of spatial form, of the Green's function [3, 7]

$$G = \frac{1}{2\pi} \iint \frac{j}{q_i} \exp[j\Phi] du dv \tag{12a}$$

$$\nabla' G = \frac{1}{2\pi} \iint \frac{\vec{g}_i}{q_i} \exp\ [j\Phi] du dv \tag{12b}$$

$$G_t = \frac{1}{2\pi} \iint \frac{j}{q_t} \exp\left[j\Phi_t\right] du dv \tag{13a}$$

$$\nabla' G_t = \frac{1}{2\pi} \iint \frac{\vec{g}_t}{q_t} \exp\left[j\Phi_t\right] du dv \tag{13b}$$

where the phase terms associated with the upper and lower medium are, respectively,

$$\mathbf{\Phi}_i = j\left[u\left(x - x'\right) + v\left(y - y'\right) - q_i|z - z'|\right] \tag{14a}$$

$$\mathbf{\Phi}_t = j\left[u\left(x - x'\right) + v\left(y - y'\right) - q_t|z - z'|\right], \tag{14b}$$

with $q_i = \sqrt{k^2 - u^2 - v^2}$; $q_t = \sqrt{k_t^2 - u^2 - v^2}$; $\vec{g}_i = \hat{x}u + \hat{y}v \mp \hat{z}q_i$; $\vec{g}_t = \hat{x}u + \hat{y}v \mp \hat{z}q_t$.

By substituting the Kirchhoff surface fields in (7a)–(7b) into (10)–(11), we obtain the estimates of the complementary fields of (8)–(9). This may be seen as a 2nd iteration of seeking the solution of the integral equations governing the surface fields using Kirchhoff fields as initial guess which is indeed a very good choice for fast convergence.

2.2.1. Far-Zone Scattered Field and Scattering Coefficients

Now, with the surface tangential field estimates available, the scattered field for q polarization at far-zone distance R is readily calculated by making use of the Stratton-Chu formula [referring to Figure 2]:

$$E_{qp}^s = KE_0 \int \left[\hat{q} \times \hat{k}_s \cdot \left(\hat{n} \times \vec{E}_p\right) + \eta\hat{q} \cdot \left(\hat{n} \times \vec{H}_p\right)\right] \exp\left[j\left(k\hat{k}_s \cdot \vec{r}\right)\right] dS \tag{15}$$

where

$$K = -\frac{jk}{4\pi R} \exp(-jkR)$$

Corresponding to the Kirchhoff and the complementary surface fields in (6a), (6b), the far-zone scattered field may also be expressed as the sum of the Kirchhoff and complementary scattered fields [3, 7]:

$$E_{qp}^s = E_{qp}^k + E_{qp}^c \tag{16}$$

where the Kirchhoff field is given by

$$E_{qp}^k = KE_0 \int f_{qp} \exp\{j\Phi\} dx dy \tag{17}$$

with the phase term $\Phi = k[(\hat{k}_s - \hat{k}_i) \cdot \vec{r}]$.

The complementary scattered field, propagating upward and downward, may be written as

$$E_{qp}^c = \frac{KE_0}{8\pi^2} \int \left\{\mathscr{F}_{qp} e^{j[\Phi_i + \vec{k}_s \cdot \vec{r} - \vec{k}_i \cdot \vec{r'}]} + \mathscr{G}_{qp} e^{j[\Phi_t + \vec{k}_s \cdot \vec{r} - \vec{k}_i \cdot \vec{r'}]}\right\} du dv dx dy dx' dy' \tag{18}$$

The Kirchhoff field coefficients f_{qp} appearing in (17) may be more explicitly written into the following form

$$f_{vv} = -\left[(1 - R_v)\,\hat{h}_s \cdot (\hat{n} \times \hat{v}_i) + (1 + R_v)\,\hat{v}_s \cdot \left(\hat{n} \times \hat{h}_i\right)\right] s_1$$

$$- (R_h + R_v)\,(\hat{v}_i \cdot \hat{t})\left[\left(\hat{h}_s \cdot \hat{d}\right)\left(\hat{n} \cdot \hat{k}_i\right) - \left(\hat{n} \cdot \hat{d}\right)\left(\hat{h}_s \cdot \hat{k}_i\right) - (\hat{v}_s \cdot \hat{t})\left(\hat{n} \cdot \hat{k}_i\right)\right] s_1 \tag{19a}$$

$$f_{vh} = \left[(1 - R_h)\,\hat{v}_s \cdot (\hat{n} \times \hat{v}_i) - (1 + R_h)\,\hat{h}_s \cdot \left(\hat{n} \times \hat{h}_i\right)\right] s_1$$

$$- (R_h + R_v)\left(\hat{h}_i \cdot \hat{d}\right)\left[\left(\hat{h}_s \cdot \hat{t}\right)\left(\hat{n} \cdot \hat{k}_i\right) - \left(\hat{n} \cdot \hat{d}\right)\left(\hat{v}_s \cdot \hat{k}_i\right) + \left(\hat{v}_s \cdot \hat{d}\right)\left(\hat{n} \cdot \hat{k}_i\right)\right] s_1 \tag{19b}$$

$$f_{hv} = \left[(1 - R_v) \, \hat{v}_s \cdot (\hat{n} \times \hat{v}_i) - (1 + R_v) \, \hat{h}_s \cdot \left(\hat{n} \times \hat{h}_i \right) \right] s_1$$

$$- (R_h + R_v) \left(\hat{v}_i \cdot \hat{t} \right) \left[\left(\hat{h}_s \cdot \hat{t} \right) \left(\hat{n} \cdot \hat{k}_i \right) - \left(\hat{n} \cdot \hat{d} \right) \left(\hat{v}_s \cdot \hat{k}_i \right) + \left(\hat{v}_s \cdot \hat{d} \right) \left(\hat{n} \cdot \hat{k}_i \right) \right] s_1 \qquad \text{(19c)}$$

$$f_{hh} = \left[(1 + R_h) \, \hat{v}_s \cdot \left(\hat{n} \times \hat{h}_i \right) + (1 - R_h) \, \hat{h}_s \cdot (\hat{n} \times \hat{v}_i) \right] s_1$$

$$- (R_h + R_v) \left(\hat{h}_i \cdot \hat{d} \right) \left[\left(\hat{h}_s \cdot \hat{d} \right) \left(\hat{n} \cdot \hat{k}_i \right) - \left(\hat{n} \cdot \hat{d} \right) \left(\hat{h}_s \cdot \hat{k}_i \right) - \left(\hat{v}_s \cdot \hat{t} \right) \left(\hat{n} \cdot \hat{k}_i \right) \right] s_1 \qquad \text{(19d)}$$

where $s_1 = \sqrt{1 + z_x^2 + z_y^2}$ accounting for surface slope.

Note that in IEM model, the terms involved $(R_h + R_v)$ in (19) are all dropped off. Keeping in mind that the Kirchhoff field coefficients f_{qp} are spatially dependent on the Fresnel reflection coefficients R_p, $p = h$, v and the surface slope term s_1. To make the integrals in (17) and (18) mathematically manageable in calculation of the average scattered power, we apply a stationary phase approximation while ignoring the edge diffraction, to obtain an estimate of the surface slopes:

$$\frac{\partial \Phi}{\partial x} = 0 \to z_x = -\frac{k_{sx} - k_x}{k_{sz} - k_z}$$

$$\frac{\partial \Phi}{\partial y} = 0 \to z_y = -\frac{k_{sy} - k_y}{k_{sz} - k_z} \qquad (20)$$

That is, the surface slopes are presumably independent of spatial variable and are approximately determined by the directions of incident and scattering waves. To further tackle the mathematical manipulations, removal of the spatial dependence of the reflection coefficient will be treated in the next section. Keeping in mind that to what extent such an estimate is valid or at least sufficiently accurate remains further investigations.

Now let us go back to the complementary scattered field, which is much more complicated to deal with. Recalled from the preceding section that the complementary scattered field is contributed from the reradiated fields that may propagate through medium 1 and medium 2, represented by upwardly and downwardly waves, the physical mechanism may be graphically represented by the field coefficients or propagators, $\mathscr{F}_{qp}$, $\mathscr{G}_{qp}$, as illustrated in Figure 2. Further dealing with the phase term involving the surface height, the propagators may be decomposed into the upward components designated by $\mathscr{F}_{qp}^+$, $\mathscr{G}_{qp}^+$ and the downward components by $\mathscr{F}_{qp}^-$, $\mathscr{G}_{qp}^-$, mathematically appearing as the absolute terms in (14), physically denoting the change of propagation velocity at different media. In the original IEM model [3, 7], the reradiated fields propagating through the lower medium is ignored, and also in calculating the coefficient $\mathscr{F}_{qp}^\pm$, a simplified phase term, $\Phi_g = j[u(x - x') + v(y - y')]$, is used by dropping off the phase term associated with the surface height, viz the term $q_i|z - z'|$. In calculating $\vec{g}_i$, $\vec{g}_t$, the z-component is ignored. Physically, this implies that the upward and downward reradiated fields are statistically canceled out [7]. Such argument holds valid more so for the cases of backscattering or when the correlation between two surface points, z, z', is electromagnetically small.

In what follows, the complete phase terms are kept and all possible propagation waves included. After straightforward but tedious mathematical manipulations, the complementary field coefficients can be obtained and put into compact forms for both the upward and downward propagations. Explicit expressions that are easy for numerical computation are given below:

$$\mathscr{F}_{vv}^\pm(u, v) = - \left(\frac{1 - R_v}{\pm q_i} \right) (1 + R_v) \, C_1 + \left(\frac{1 - R_v}{\pm q_i} \right) (1 - R_v) \, C_2 + \left(\frac{1 - R_v}{\pm q_i} \right) (1 + R_v) \, C_3$$

$$+ \left(\frac{1 + R_v}{\pm q_i} \right) (1 - R_v) \, C_4 + \left(\frac{1 + R_v}{\pm q_i} \right) (1 + R_v) \, C_5 + \left(\frac{1 + R_v}{\pm q_i} \right) (1 - R_v) \, C_6 \qquad \text{(21a)}$$

$$\mathscr{G}_{vv}^\pm(u, v) = \left(\frac{(1 + R_v) \, \mu_r}{\pm q_t} \right) (1 + R_v) \, C_{1t} - \left(\frac{1 + R_v}{\pm q_t} \right) (1 - R_v) \, C_{2t} - \left(\frac{1 + R_v}{\pm q_t \varepsilon_r} \right) (1 + R_v) \, C_{3t}$$

$$- \left(\frac{(1 - R_v) \, \varepsilon_r}{\pm q_t} \right) (1 - R_v) \, C_{4t} - \left(\frac{1 - R_v}{\pm q_t} \right) (1 + R_v) \, C_{5t} - \left(\frac{1 - R_v}{\pm q_t \mu_r} \right) (1 - R_v) \, C_{6t} \qquad \text{(21b)}$$

$$\mathscr{F}_{hh}^{\pm}(u,v) = \left(\frac{1-R_h}{\pm q_i}\right)(1+R_h)\,C_1 - \left(\frac{1-R_h}{\pm q_i}\right)(1-R_h)\,C_2 - \left(\frac{1-R_h}{\pm q_i}\right)(1+R_h)\,C_3$$

$$- \left(\frac{1+R_h}{\pm q_i}\right)(1-R_h)\,C_4 - \left(\frac{1+R_h}{\pm q_i}\right)(1+R_h)\,C_5 - \left(\frac{1+R_h}{\pm q_i}\right)(1-R_h)\,C_6 \quad (21c)$$

$$\mathscr{G}_{hh}^{\pm}(u,v) = -\left(\frac{(1+R_h)\,\varepsilon_r}{\pm q_t}\right)(1+R_h)\,C_{1t} + \left(\frac{1+R_h}{\pm q_t}\right)(1-R_h)\,C_{2t} - \left(\frac{1+R_h}{\pm q_t \mu_r}\right)(1+R_h)\,C_{3t}$$

$$+ \left(\frac{(1+R_h)\,\mu_r}{\pm q_t}\right)(1-R_h)\,C_{4t} + \left(\frac{1-R_h}{\pm q_t}\right)(1+R_h)\,C_{5t} - \left(\frac{1-R_h}{\pm q_t \varepsilon_r}\right)(1-R_h)\,C_{6t} \quad (21d)$$

$$\mathscr{F}_{hv}^{\pm}(u,v) = \left(\frac{1-R}{\pm q_i}\right)(1+R)\,B_1 + \left(\frac{1-R}{\pm q_i}\right)(1-R)\,B_2 - \left(\frac{1-R}{\pm q}\right)(1+R)\,B_3$$

$$+ \left(\frac{1+R}{\pm q_i}\right)(1-R)\,B_4 + \left(\frac{1+R}{\pm q_i}\right)(1+R)\,B_5 - \left(\frac{1+R}{\pm q_i}\right)(1-R)\,B_6 \quad (21e)$$

$$\mathscr{G}_{hv}^{\pm}(u,v) = -\left(\frac{(1+R)\,\mu_r}{\pm q_t}\right)(1+R)\,B_{1t} + \left(\frac{1+R}{\pm q_t}\right)(1-R)\,B_{2t} + \left(\frac{1+R}{\pm q_t \varepsilon_r}\right)(1+R)\,B_{3t}$$

$$- \left(\frac{(1-R)\,\varepsilon_r}{\pm q_t}\right)(1-R)\,B_{4t} + \left(\frac{1-R}{\pm q_t}\right)(1+R)\,B_{5t} + \left(\frac{1-R}{\pm q_t \mu_r}\right)(1-R)\,B_{6t} \quad (21f)$$

$$\mathscr{F}_{vh}^{\pm}(u,v) = \left(\frac{1+R}{\pm q_i}\right)(1-R)\,B_1 - \left(\frac{1+R}{\pm q_i}\right)(1+R)\,B_2 - \left(\frac{1+R}{\pm q_i}\right)(1-R)\,B_3$$

$$+ \left(\frac{1-R}{\pm q_i}\right)(1+R)\,B_4 + \left(\frac{1-R}{\pm q_i}\right)(1-R)\,B_5 + \left(\frac{1-R}{\pm q_i}\right)(1+R)\,B_6 \quad (21g)$$

$$\mathscr{G}_{vh}^{\pm}(u,v) = -\left(\frac{(1-R)\,\varepsilon_r}{\pm q_t}\right)(1-R)\,B_{1t} + \left(\frac{1-R}{\pm q_t}\right)(1+R)\,B_{2t} + \left(\frac{1-R}{\pm q_t \mu_r}\right)(1-R)\,B_{3t}$$

$$- \left(\frac{(1+R)\,\mu_r}{\pm q_t}\right)(1+R)\,B_{4t} - \left(\frac{1+R}{\pm q_t}\right)(1-R)\,B_{5t} - \left(\frac{1+R}{\pm q_t \varepsilon_r}\right)(1+R)\,B_{6t} \quad (21h)$$

For cross polarizations, we use an approximate reflection coefficient by taking the average of the reflection coefficients of horizontal and vertical polarizations: $R \approx \frac{1}{2}(R_h + R_v)$ [3]. The coefficients C, B, C_t B_t appearing in (21) are given in Appendix A. Note that the coefficients C_t B_t for the lower or transmitted medium have similar forms to C and B with q being simply replaced by q_t.

It is readily realized that for downward radiation, the field coefficients are obtained by replacing k_z by $-k_z$, and k_{tz} by $-k_{tz}$. That is, $\mathscr{F}_{qp}^- = \mathscr{F}_{qp}^+(k_x, k_y, -k_z)$, $\mathscr{G}_{qp}^- = \mathscr{G}_{qp}^+(k_x, k_y, -k_{tz})$.

With the scattered fields calculated, we perform ensemble averaging to compute the scattered power and scattering coefficient. To gain more physical insights into the field interactions that produce the average power, the following expression for the incoherent average power is written as a sum of three terms: the Kirchhoff power, the cross power due by the Kirchhoff field and the complementary power:

$$P_{qp}^s = \left\langle E_{qp}^s E_{qp}^{s*} \right\rangle - \left\langle E_{qp}^s \right\rangle \left\langle E_{qp}^{s*} \right\rangle = \left\langle E_{qp}^k E_{qp}^{k*} \right\rangle - \left\langle E_{qp}^k \right\rangle \left\langle E_{qp}^{k*} \right\rangle$$

$$+ 2\mathscr{R}e\left[\left\langle E_{qp}^c E_{qp}^{k*} \right\rangle - \left\langle E_{qp}^c \right\rangle \left\langle E_{qp}^{k*} \right\rangle \right] + \left\langle E_{qp}^c E_{qp}^{c*} \right\rangle - \left\langle E_{qp}^c \right\rangle \left\langle E_{qp}^{c*} \right\rangle \triangleq P_{qp}^k + P_{qp}^{kc} + P_{qp}^c \quad (22)$$

where $\langle\,\rangle$ denotes the ensemble average over the randomly rough surface $z(x, y)$, and $*$ is the complex conjugation operator. Referring to Figure 3, it is readily recognized that the cross power is the result of the interactions between the Kirchhoff field and the complementary field, involved by 4 terms — 2 accounting for the upper medium propagation and another 2 for the lower medium:

$$P_{qp}^{kc} = P_{qp|\mathscr{F}_{qp}^+}^{kc} + P_{qp|\mathscr{F}_{qp}^-}^{kc} + P_{qp|\mathscr{G}_{qp}^+}^{kc} + P_{qp|\mathscr{G}_{qp}^-}^{kc} \quad (23)$$

Similarly, the radiated power by the complementary field itself is mutually generated by reradiation fields from every point on the surface and thus consists of sixteen terms resulting from interactions of
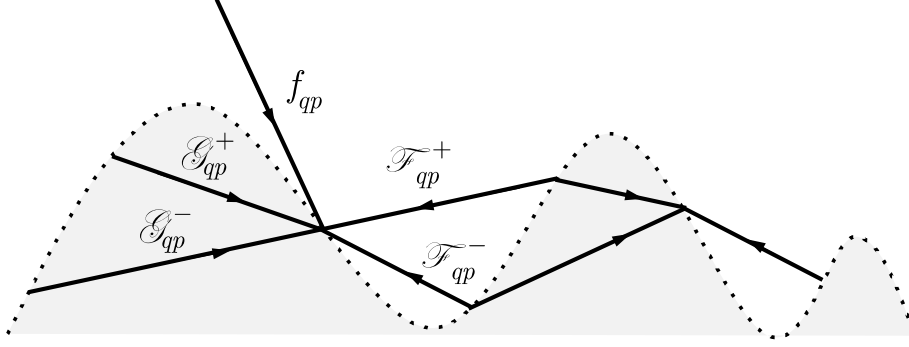
Figure 3. Interactions among Kirchhoff fields and complementary fields to generate the scattering power given in Equation (24).

2 upward fields and 2 downward fields propagating through medium 1 and medium 2 [see Figure 3]:

$$
\begin{aligned}
P_{qp}^c = {} & P_{qp|\mathscr{F}_{qp}^+\mathscr{F}_{qp}^+}^c + P_{qp|\mathscr{F}_{qp}^+\mathscr{F}_{qp}^-}^c + P_{qp|\mathscr{F}_{qp}^+\mathscr{G}_{qp}^+}^c + P_{qp|\mathscr{F}_{qp}^+\mathscr{G}_{qp}^-}^c \\
& + P_{qp|\mathscr{F}_{qp}^-\mathscr{F}_{qp}^+}^c + P_{qp|\mathscr{F}_{qp}^-\mathscr{F}_{qp}^-}^c + P_{qp|\mathscr{F}_{qp}^-\mathscr{G}_{qp}^+}^c + P_{qp|FG_{qp}^-\mathscr{G}_{qp}^-}^c \\
& + P_{qp|\mathscr{G}_{qp}^+\mathscr{F}_{qp}^+}^c + P_{qp|\mathscr{G}_{qp}^+\mathscr{F}_{qp}^-}^c + P_{qp|\mathscr{G}_{qp}^+\mathscr{G}_{qp}^+}^c + P_{qp|\mathscr{G}_{qp}^+\mathscr{G}_{qp}^-}^c \\
& + P_{qp|\mathscr{G}_{qp}^-\mathscr{F}_{qp}^+}^c + P_{qp|\mathscr{G}_{qp}^-\mathscr{F}_{qp}^-}^c + P_{qp|\mathscr{G}_{qp}^-\mathscr{G}_{qp}^+}^c + P_{qp|\mathscr{G}_{qp}^-\mathscr{G}_{qp}^-}^c
\end{aligned}
\tag{24}
$$

Now by substituting the Kirchhoff field given in Equation (17) and the complementary field given in Equation (18) into Equation (22) and carrying out the ensemble averages, we obtain an explicit expression of the incoherent average power. When the medium is very lossy, contributions from the lower medium propagation is expected to be small. However, in general, all modes must be included to get a more complete scattered power, as claimed in [19]. After some algebraic manipulations and arrangements, we can reach the final expression of a relatively compact form as:

$$
\sigma_{qp}^s = \frac{k^2}{2} \exp\left[-\sigma^2\left(k_{iz}^2 + k_{sz}^2\right)\right] \sum_{n=1}^{\infty} \frac{\sigma^{2n}}{n!} |\mathscr{I}_{qp}^n|^2 \mathbf{W}^{(n)}\left(k_{sx} - k_{ix}, k_{sy} - k_{iy}\right)
\tag{25}
$$

where

$$
\begin{aligned}
\mathscr{I}_{qp}^n = {} & (k_{sz} + k_{iz})^n f_{qp} \exp\left(-\sigma^2 k_{iz} k_{sz}\right) \\
& + \frac{1}{4}\Big\{ \mathscr{F}_{qp}^+(-k_{ix}, -k_{iy})(k_{sz} - k_{iz})^n \exp\left[-\sigma^2\left(k_{iz}^2 - k_{iz}(k_{sz} - k_{iz})\right)\right] \\
& + \mathscr{F}_{qp}^+(-k_{sx}, -k_{sy})(k_{sz} + k_{iz})^n \exp\left[-\sigma^2\left(k_{iz}^2 - k_{iz}(k_{sz} - k_{iz})\right)\right] \\
& + \mathscr{F}_{qp}^-(-k_{sx}, -k_{sy})(k_{sz} - k_{iz})^n \exp\left[-\sigma^2\left(k_{iz}^2 + k_{iz}(k_{sz} - k_{iz})\right)\right] \\
& + \mathscr{G}_{qp}^+(-k_{ix}, -k_{iy})(k_{sz} - k_{tz})^n \exp\left[-\sigma^2\left(k_{tz}^2 - k_{tz}(k_{sz} - k_{iz})\right)\right] \\
& + \mathscr{G}_{qp}^-(-k_{ix}, -k_{iy})(k_{sz} + k_{tz})^n \exp\left[-\sigma^2\left(k_{tz}^2 + k_{tz}(k_{sz} - k_{iz})\right)\right] \\
& + \mathscr{G}_{qp}^+(-k_{sx}, -k_{sy})(k_{sz} + k_{tz})^n \exp\left[-\sigma^2\left(k_{tz}^2 - k_{tz}(k_{sz} - k_{iz})\right)\right] \\
& + \mathscr{G}_{qp}^-(-k_{sx}, -k_{sy})(k_{sz} - k_{tz})^n \exp\left[-\sigma^2\left(k_{tz}^2 + k_{tz}(k_{sz} - k_{iz})\right)\right] \Big\}
\end{aligned}
\tag{26}
$$

and $\mathbf{W}^{(n)}(k_{sx} - k_{ix}, k_{sy} - k_{iy})$ is the surface roughness spectrum of the surface related to the nth power of the surface correlation function by two-dimensional Fourier transform, assuming that the surface height is Gaussian distribution, and σ is surface *rms* height. In all numerical computations in this paper, we use exponential correlation with correlation length ℓ. When the surface roughness is very large, the use of (25) might be computationally slow to reach convergence. As for the surface roughness spectrum, a generalized power law spectrum was proposed to characterize a broad range of rough surface statistics [22]. For non-Gaussian surface height distributions with non-symmetry, higher order statistics, e.g., bispectral, may be included [8].

2.3. A New Transition Function for Fresnel Reflection Coefficients

The Fresnel reflection coefficient for a homogenous rough surface is dependent on the local incidence angle, which is determined by the incident direction and surface unit normal. In modeling the wave scattering, in order to remove the spatial dependence of the reflection coefficient, it is a common practice to approximate the local incident angle either by the incident angle for a slightly rough surface or by the specular angle. Such approximation, however, leads to an unpredictable error for the local incident angle which is random in nature across the rough surface. A transition model was proposed [11] to fix such deficiency. It is necessary to generalize the transition function so that the local angle variation is accounted for. This is important for a scattering model to cover a wider range of surface roughness. Recalling that the scattering coefficient may be decomposed into three terms, recognized as Kirchhoff, cross, and complementary terms: $\sigma_{qp}^o = \sigma_{qp}^k + \sigma_{qp}^{kc} + \sigma_{qp}^c$. The transition model takes two extremes of the form [11]

$$R_p(T) = R_p(\theta_i) + [R_p(\theta_{sp}) - R_p(\theta_i)]\gamma_p \tag{27}$$

where θ_i is the incidence angle, θ_{sp} the specular angle, and the transition function is defined as

$$\gamma_p = 1 - \frac{S_p}{S_p^o} \tag{28a}$$

with

$$S_p = \frac{\sigma_{pp}^c\big|_{R_p=R_p(0)}}{\sigma_{pp}^o\big|_{R_p=R_p(0)}}, \tag{28b}$$

$$S_p^o = \lim_{k\sigma\to 0} \frac{\sigma_{pp}^c\big|_{R_p=R_p(0)}}{\sigma_{pp}^o\big|_{R_p=R_p(0)}} \tag{28c}$$

Note that $\lim_{k_\sigma\to 0} \sigma_{pp}^o = a+b+c$, $\lim_{k_\sigma\to 0} \sigma_{pp}^c = c$, with the coefficients a, b, c, corresponding to the Kirchhoff, cross and complementary terms, respectively. Under the framework of the AIEM model, the three terms are given in Appendix B.

The Fresnel reflection coefficients for horizontally and vertically polarized waves are, respectively

$$R_h = \frac{\mu_t k \cos\theta_i - \mu_0 k_{tz}}{\mu_t k \cos\theta_i + \mu_0 k_{tz}}, \tag{29a}$$

$$R_v = \frac{\varepsilon_0 k_{tz} - \varepsilon_t k \cos\theta_i}{\varepsilon_t k \cos\theta_i + \varepsilon_0 k_{tz}}, \tag{29b}$$

where

$$k_{tz} = \mathscr{R}e\{k_{tz}\} + j\mathscr{I}m\{k_{tz}\} \tag{29c}$$

with

$$\mathscr{R}e\{k_{tz}\} = \frac{1}{\sqrt{2}}\left[\mathscr{R}e\{k_t^2\} - k^2\sin^2\theta_i + \sqrt{\left(\mathscr{R}e\{k_t^2\} - k^2\sin^2\theta_i\right)^2 + \left(\mathscr{I}m\{k_t^2\}\right)^2}\right]^{1/2} \tag{29d}$$

$$\mathscr{I}m\{k_{tz}\} = -\frac{1}{\sqrt{2}}\left[-\left(\mathscr{R}e\{k_t^2\} - k^2\sin^2\theta_i\right) + \sqrt{\left(\mathscr{R}e\{k_t^2\} - k^2\sin^2\theta_i\right)^2 + \left(\mathscr{I}m\{k_t^2\}\right)^2}\right]^{1/2} \tag{29e}$$

2.3.1. Numerical Illustrations

In what follows, we shall demonstrate the use of the update transition function for Fresnel reflection coefficient, with Geometric Optics model (GOM) as a reference. Figure 4 displays a set of bistatic scattering coefficients for a rough surface with dielectric constants of $\varepsilon_r = 10 + j0.05$. The incident angle and scattering angle at fixed at $\theta_i = 20°$, $\theta_s = 40°$ with a surface roughness of $k_\ell = 6.28$, $k_\sigma = 0.628$. At this surface roughness scale, the first order SPM is not valid. The azimuthal angular behavior of AIEM and GOM predictions are closely matched with the updated transition model perfectly following that of

GOM at the location of dip of the scattering coefficient. Now to see the impact of dielectric constant, we set the surface roughness to a very large of $k_\ell = 7.5$, $k_\sigma = 2.8$, for dielectric constants of $\varepsilon_r = 4 - j0.3$, $9 - j1.8$, 16, $40 - j3$. The incident angle and scattering angle are fixed at $\theta_i = 50°$ and $\theta_s = 30°$. From
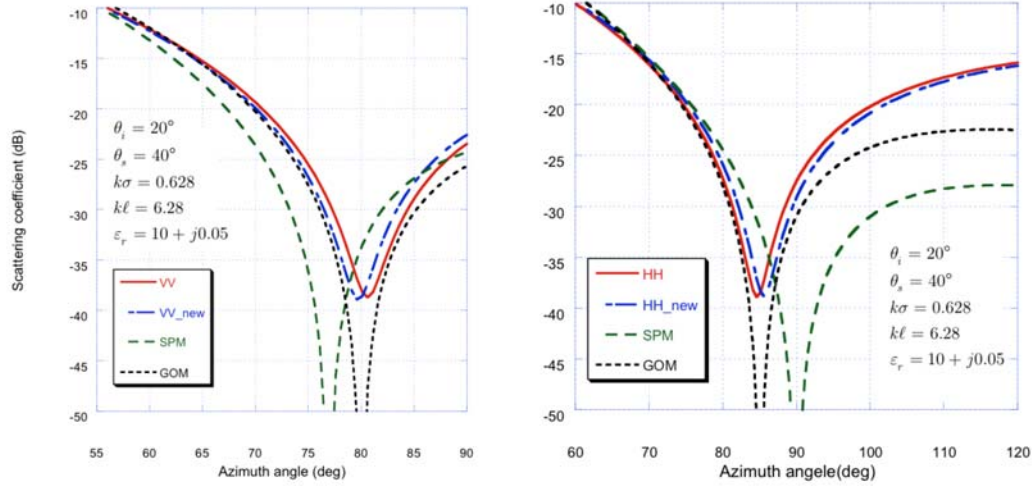
Figure 4. Bistatic scattering coefficient with dielectric constants $\varepsilon_r = 10 + j0.05$ and surface roughness of $k_\sigma = 0.628$, $k_\ell = 6.28$. The incident angle and scattering angle are fixed at $\theta_i = 20°$, $\theta_s = 40°$. The GOM and SPM models are plotted for reference.
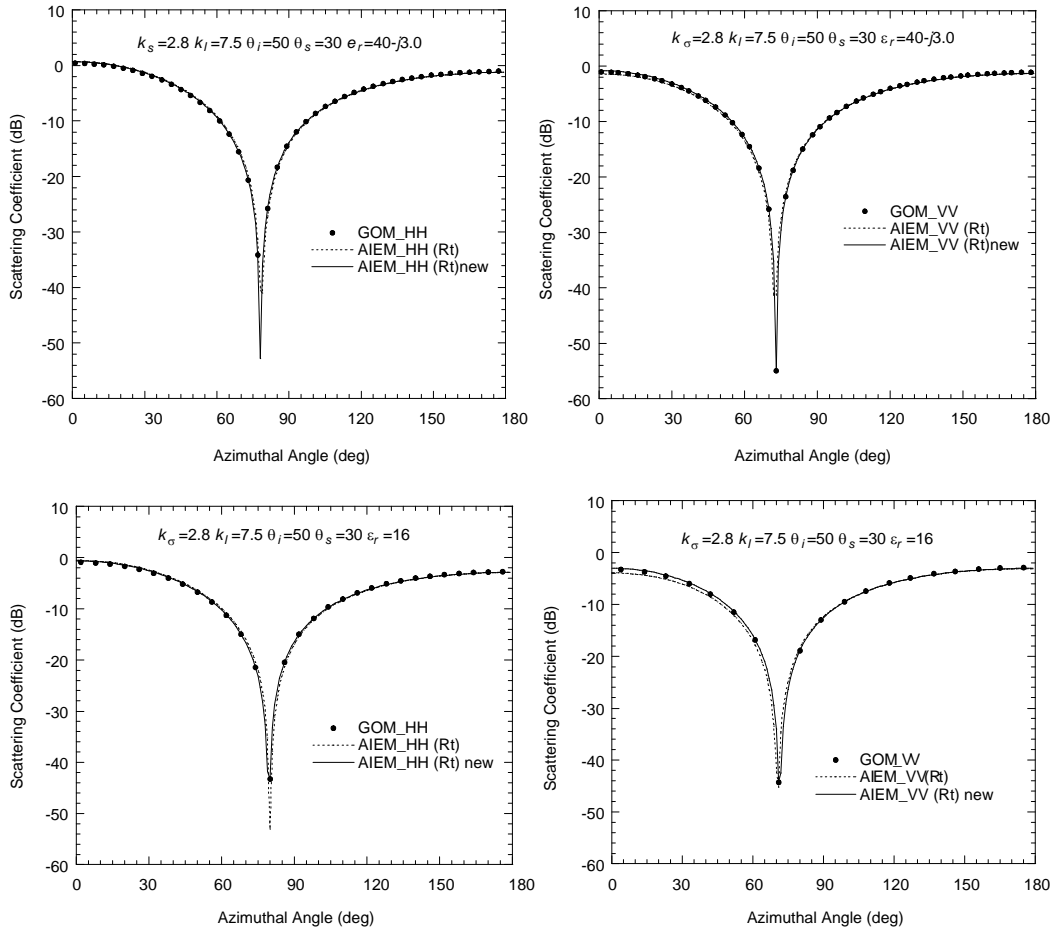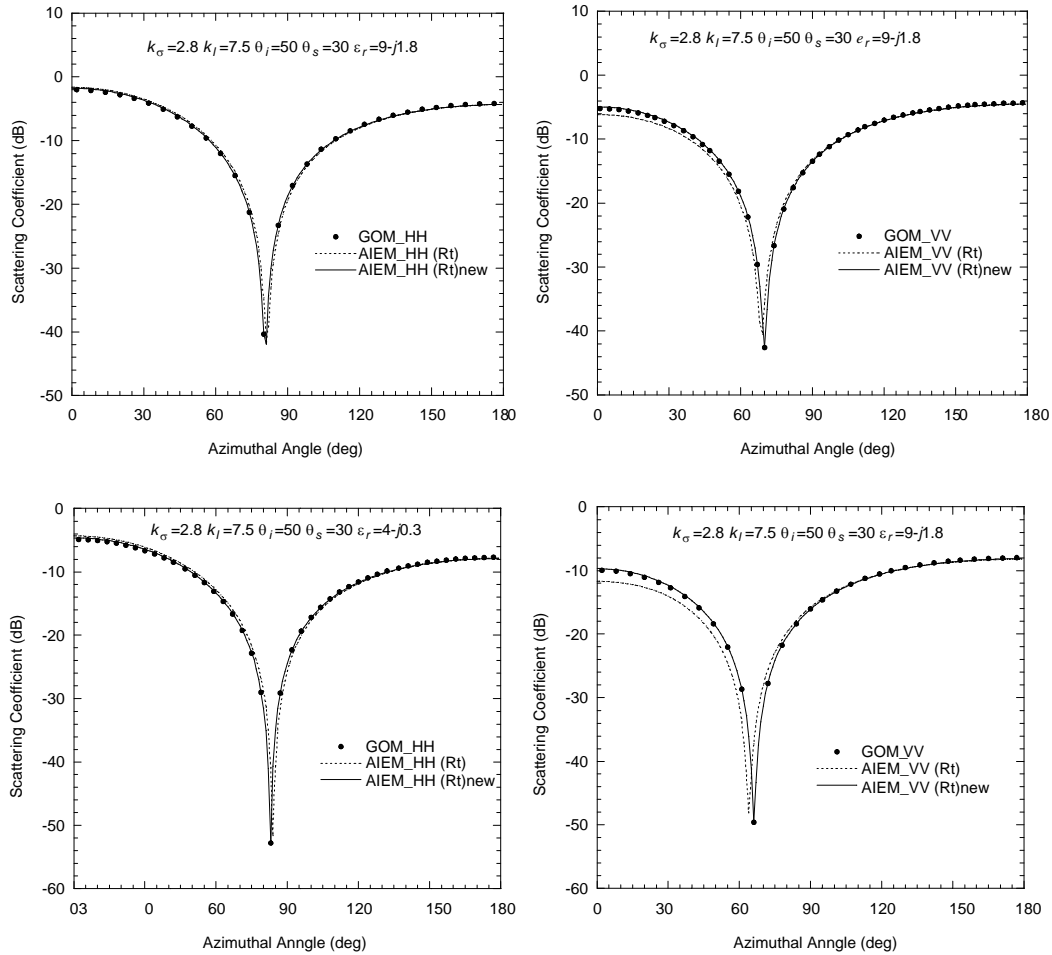
Figure 5. Scattering coefficients calculated by AIEM with old and new transition model in reflection coefficient for dielectric constants $\varepsilon_r = 4 - j0.3$, $9 - j1.8$, 16, $40 - j3$. The incident angle and scattering angle fixed at $\theta_i = 50°$, $\theta_s = 30°$ with a surface roughness of $k_s = 2.5$, $k_l = 7.5$.

Figure 5, it is observed that the difference between the use of old transition model and new one in AIEM becomes larger as the surface dielectric constant decreases. At large dielectric, essentially there is no difference between the two models, as expected. Also it is clear that the transition model has more impact on the vertical polarization than on horizontal polarization. With the use of the updated transition model, the azimuthal angular behavior perfectly follows that of GOM. The prediction of the dip in the azimuthal plane is apparently dislocated for the old transition model.

At this point, it is interesting to further exam the effect of the surface dielectric property on bistatic scattering. Focus is placed on the lossy effect, namely, the magnitude of the imaginary part of the dielectric constant. We use the same parameters in Figure 4, except at smaller roughness of $k_\sigma = 0.314$, $k_\ell = 3.14$ and increasing the loss tangent. Results are plotted in Figure 6, where three sets of bistatic scattering coefficients are shown, namely predicted by AIEM, GOM, and SPM models. It is clearly seen that as the dielectric loss increases, the dip in azimuthal plane is changed not only for its magnitude, but also for its angular width. The dislocation of the dip in azimuth scattering plane by SPM predictions is understood for their invalid at this roughness scale. The more the surface is lossy, the shallower and wider the dip becomes. Further verification of this behavior and possible physical mechanisms behind it may be necessary by means of either full-blown numerical simulation or laboratory measurement, or better both. For very lossy surface, numerical simulation will be a very challenging work. Nevertheless, at this point, the presented three examples persistently explain the need of an updated transition model for reflection coefficient for more accurate prediction of bistatic
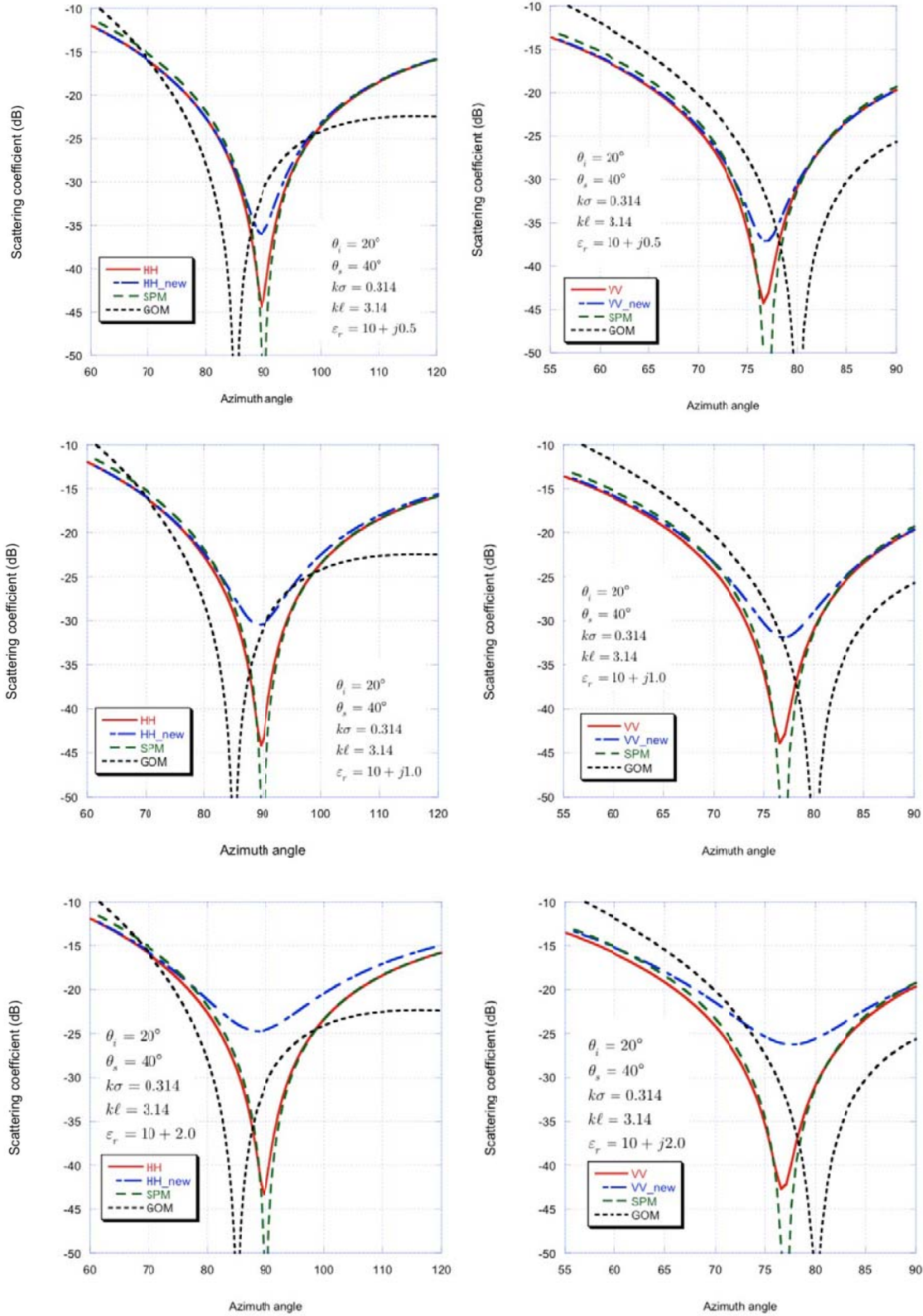
Figure 6. Effects of dielectric loss properties with incident angle and scattering angle fixed at $\theta_i = 20°$, $\theta_s = 40°$ and surface roughness of $k_\sigma = 0.314$, $k_\ell = 3.14$. The dielectric constants are $\varepsilon_r = 10 + j0.5$, $\varepsilon_r = 10 + j1.0$, $\varepsilon_r = 10 + j2.0$.

scattering. To further illustrate the model performance, comparisons with numerical simulations and experimental data, all from published literatures, are made in the following section.

3. COMPARISON WITH NUMERICAL SIMULATIONS

Though only limited simulations are available, the prediction of scattering coefficient in scattering plane between the present model and numerical results of SSA (Small Slope Approximation) and MoM (method of moment) is shown in Figure 7. The simulation data are adopted from [23] for a Gaussian correlated surface with $\varepsilon_r = 4 - j1$; $k_\sigma = 0.5$, $k_\ell = 3.0$ at incident angle of 30 degrees and scattering angle between -60 and 60 degrees. Obviously, all the three predictions are quite close to each other except at larger scattering angle. There is a dip in specular direction shown by MoM and SSA, but not by AIEM. Doubling the surface roughness, results are given in Figure 8 from which we can see that the angular trends by three predictions are similar to those in Figure 7. The dip in specular direction is now largely shallow because of more roughness.
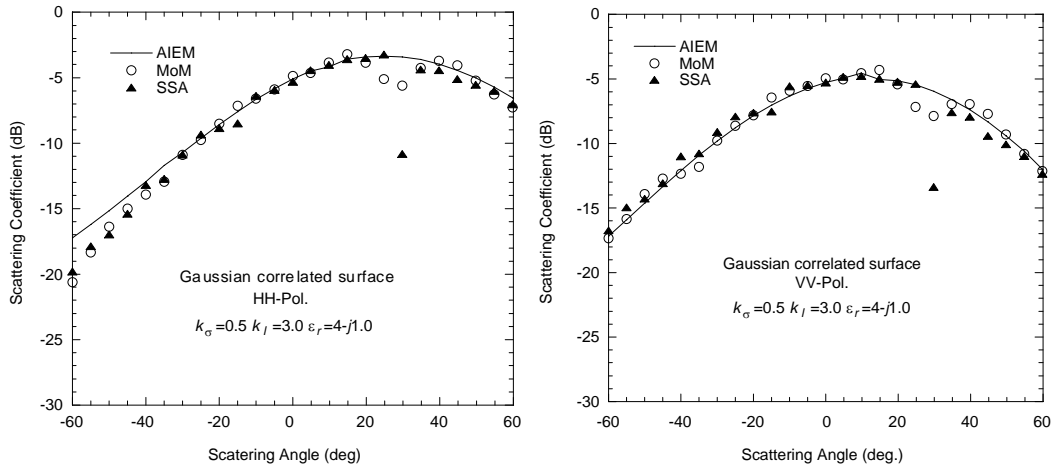
Figure 7. Comparison of scattering coefficient between AIEM model and numerical results of MoM and SSA for both horizontal and vertical polarization for a Gaussian correlated surface with $\varepsilon_r = 4 - j1$; $k_\sigma = 0.5$, $k_\ell = 3.0$, and incident angle of 30 degrees.
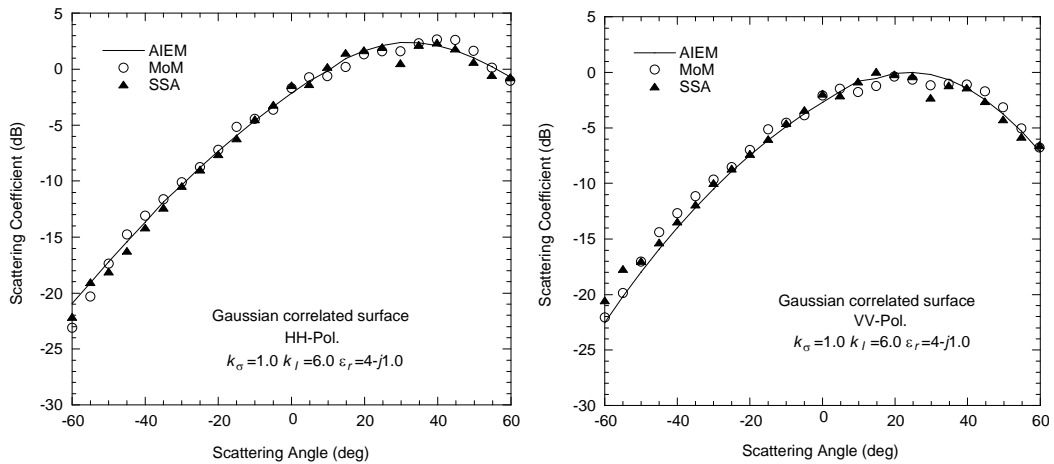
Figure 8. Comparison of scattering coefficient between AIEM model and numerical results of MoM and SSA for both horizontal and vertical polarization for a Gaussian correlated surface with $\varepsilon_r = 4 - j1$; $k_\sigma = 1.0$, $k_\ell = 6.0$, and incident angle of 30 degrees.

4. SUMMARY

This paper provides extensions of an Advanced Integral Equation Model (AIEM) for rough surface scattering. A framework of the model development is outlined, followed by giving model expression. A complete Kirchhoff field is included. Accordingly, a transition function for Fresnel reflection coefficients is also derived. Numerical illustrations are given for bistatic scattering, by comparisons with numerical simulations and experimental measurements. All the model coefficients are written to give their explicit forms for the ease of numerical computation. It is believed that the AIEM presented here provides very accurate predictions of bistatic scattering, which is becoming more interesting for remote sensing of terrain and sea. Therefore, it is suggested that the AIEM model, covering a very wide range of surface property and observation geometry, offers a useful tool for the interpretation of the scattering mechanisms, and perhaps more practically, for surface parameters retrieval. As a final note, because all expressions in the model are in algebraic form, computational effort is not an issue.

APPENDIX A.

In this appendix, we give the explicit expressions of upward and downward reradiation coefficients appearing in Equations (21a)∼(21h).

$$C_1 = \cos\left(\phi_s - \phi\right)\left[1 - \frac{(k_{sx} + u)\,(k_x + u)}{(k_{sz} - q)\,(k_z + q)}\right] - \sin\left(\phi_s - \phi\right)\frac{(k_z + u)\,(k_{sy} + v)}{(k_{sz} - q)\,(k_z - q)} \tag{A1}$$

$$
\begin{aligned}
C_2 = & -\cos\left(\phi_s - \phi\right)\left[-q\cos\theta + \frac{u\cos\theta\,(k_{sx} + u)}{k_{sz} - q} - \frac{q_1\sin\theta\,(k_x + u)}{k_z + q} + \frac{u\sin\theta\,(k_{sx} + u)\,(k_x + u)}{(k_{sz} - q)\,(k_z + q)}\right. \\
& \left. - \frac{v\cos\theta\,(k_y + v)}{k_z + q} + \frac{v\sin\theta\,(k_{sx} + u)\,(k_y + v)}{(k_{sz} - q)\,(k_z + q)}\right] \\
& + \sin\left(\phi_s - \phi\right)\left[-\frac{u\cos\theta\,(k_{sy} + v)}{k_{sz} - q} - \frac{u\sin\theta\,(k_x + u)\,(k_{sy} + v)}{(k_{sz} - q)\,(k_z + q)} + \frac{q_1\sin\theta\,(k_y + v)}{k_z + q}\right. \\
& \left. - \frac{u\cos\theta\,(k_y + v)}{k_z + q} - \frac{v\sin\theta\,(k_{sy} + v)\,(k_y + v)}{(k_{sz} - q)\,(k_z + q)}\right]
\end{aligned}
\tag{A2}
$$

$$
\begin{aligned}
C_3 = & \frac{-(k_z + q)\sin\theta + (k_x + u)\cos\theta}{(k_{sz} - q)\,(k_z + q)} \\
& + \frac{[k_{sx}q\cos\left(\phi_s - \phi\right) + k_{sy}q\sin\left(\phi_s - \phi\right) + k_{sz}u\cos\left(\phi_s - \phi\right) + k_{sz}v\sin\left(\phi_s - \phi\right)]}{(k_{sz} - q)\,(k_z + q)}
\end{aligned}
\tag{A3}
$$

$$
\begin{aligned}
C_4 = & \cos\theta_s\sin\left(\phi_s - \phi\right)\left[\frac{\sin\theta\,(k_y + v)}{k_z + q} + \frac{\cos\theta\,(k_{sx} + u)\,(k_y + v)}{(k_{sz} - q)\,(k_z + q)}\right] \\
& + \cos\theta_s\cos\left(\phi_s - \phi\right)\left[\cos\theta + \frac{\sin\theta\,(k_x + u)}{k_z + q} - \frac{\cos\theta\,(k_{sy} + v)\,(k_y + v)}{(k_{sz} - q)\,(k_z + q)}\right] \\
& + \sin\theta_s\left[\frac{\cos\theta\,(k_{sx} + u)}{k_{sz} - q} + \frac{\sin\theta\,(k_{sx} + u)\,(k_x + u)}{(k_{sz} - q)\,(k_z + q)} + \frac{\sin\theta\,(k_{sy} + v)\,(k_y + v)}{(k_{sz} - q)\,(k_z + q)}\right]
\end{aligned}
\tag{A4}
$$

$$
\begin{aligned}
C_5 = & -\cos\theta_s\sin\left(\phi_s - \phi\right)\left[\frac{(k_{sx} + u)\,v}{k_{sz} - q} + \frac{(k_x + u)\,v}{k_z + q}\right] \\
& - \cos\theta_s\cos\left(\phi_s - \phi\right)\left[q + \frac{(k_x + u)\,u}{k_z + q} - \frac{(k_{sy} + v)\,v}{k_{sz} - q}\right]
\end{aligned}
$$

$$-\sin\theta_s\left[\frac{q_1\left(k_{sx}+u\right)}{k_{sz}-q}+\frac{u\left(k_{sx}+u\right)\left(k_x+u\right)}{\left(k_{sz}-q\right)\left(k_z+q\right)}+\frac{v\left(k_{sy}+v\right)\left(k_x+u\right)}{\left(k_{sz}-q\right)\left(k_z+q\right)}\right] \tag{A5}$$

$$C_6=\cos\theta_s\sin\left(\phi_s-\phi\right)\left[\frac{q\left(k_{sx}+u\right)\left(k_y+v\right)}{\left(k_{sz}-q\right)\left(k_z+q\right)}+\frac{u\left(k_y+v\right)}{k_z+q}\right]$$

$$-\cos\theta_s\cos\left(\phi_s-\phi\right)\left[\frac{q_1\left(k_{sy}+u\right)\left(k_y+v\right)}{\left(k_{sz}-q\right)\left(k_z+q\right)}+\frac{v\left(k_y+v\right)}{k_z+q}\right]$$

$$+\sin\theta_s\left[\frac{u\left(k_{sy}+v\right)\left(k_y+v\right)}{\left(k_{sz}-q\right)\left(k_z+q\right)}-\frac{u\left(k_{sx}+u\right)\left(k_x+v\right)}{\left(k_{sz}-q\right)\left(k_z+q\right)}\right] \tag{A6}$$

$$B_1=\cos\theta_s\sin\left(\phi_s-\phi\right)\left[1-\frac{q\left(k_{sx}+u\right)\left(k_x+u\right)}{\left(k_{sz}-q\right)\left(k_z+q\right)}\right]$$

$$+\cos\theta_s\cos\left(\phi_s-\phi\right)\frac{\sin\theta_s k_{sx}+\left(k_{sy}+v\right)}{k_{sz}-q}\frac{\left(k_x+u\right)\left(k_{sy}+v\right)}{\left(k_{sz}-q\right)\left(k_z+q\right)} \tag{A7}$$

$$B_2=\cos\theta_s\sin\left(\phi_s-\phi\right)\left[q\cos\theta-\frac{u\cos\theta\left(k_{sx}+u\right)}{k_{sz}-q}+\frac{q\sin\theta\left(k_x+u\right)}{k_z+q}\right.$$

$$\left.-\frac{u\sin\theta\left(k_{sx}+u\right)\left(k_x+u\right)}{\left(k_{sz}-q\right)\left(k_z+q\right)}+\frac{v\cos\theta\left(k_y+v\right)}{k_z+q}-\frac{v\sin\theta\left(k_{sx}+u\right)\left(k_x+u\right)}{\left(k_{sz}-q\right)\left(k_z+q\right)}\right]$$

$$+\sin\theta_s\left[\frac{q\cos\theta\left(k_{sy}+v\right)}{k_{sz}-q}+\frac{q_1\sin\theta\left(k_x+u\right)\left(k_{sy}+v\right)}{\left(k_{sz}-q\right)\left(k_z+q\right)}+\frac{q_1\sin\theta\left(k_{sx}+u\right)\left(k_y+v\right)}{\left(k_{sz}-q\right)\left(k_z+q\right)}\right.$$

$$\left.+\frac{u\cos\theta\left(k_{sx}+u\right)\left(k_y+v\right)}{\left(k_{sz}-q\right)\left(k_z+q\right)}+\frac{v\cos\theta\left(k_{sy}+v\right)\left(k_y+v\right)}{\left(k_{sz}-q\right)\left(k_z+q\right)}\right]$$

$$+\cos\theta_s\cos\left(\phi_s-\phi\right)\left[\frac{q\cos\theta\left(k_{sy}+v\right)}{k_{sz}-q}+\frac{u\sin\theta\left(k_x+u\right)\left(k_{sy}+v\right)}{\left(k_{sz}-q\right)\left(k_z+q\right)}-\frac{q\sin\theta\left(k_y+v\right)}{k_z+q}\right.$$

$$\left.+\frac{u\cos\theta\left(k_y+v\right)}{k_z+q}+\frac{v\sin\theta\left(k_y+v\right)\left(k_{sy}+v\right)}{\left(k_{sz}-q\right)\left(k_z+q\right)}\right] \tag{A8}$$

$$B_3=-\cos\theta_s\sin\left(\phi_s-\phi\right)\left[\frac{q\sin\theta\left(k_{sx}+u\right)}{k_{sz}-q}+u\sin\theta-\frac{q\cos\theta\left(k_{sx}+u\right)\left(k_x+u\right)}{\left(k_{sz}-q\right)\left(k_z+q\right)}-\frac{u\cos\theta\left(k_x+u\right)}{k_z+q}\right]$$

$$+\cos\theta_s\cos\left(\phi_s-\phi\right)\left[\frac{q_1\sin\theta\left(k_{sy}+v\right)}{k_{sz}-q}+v\sin\theta-\frac{q_1\cos\theta\left(k_{sy}+v\right)\left(k_x+u\right)}{\left(k_{sz}-q_1\right)\left(k_z+q\right)}-\frac{v\cos\theta\left(k_x+u\right)}{k_z+q}\right]$$

$$-\sin\theta_s\left[\frac{u\sin\theta\left(k_{sy}+v\right)}{k_z-q}-\frac{u\cos\theta\left(k_{sy}+v\right)\left(k_x+u\right)}{\left(k_{sz}-q\right)\left(k_z+q\right)}-\frac{v\sin\theta\left(k_{sx}+u\right)}{k_{sz}-q}+\frac{v\cos\theta\left(k_{sx}+u\right)\left(k_x+u\right)}{\left(k_{sz}-q\right)\left(k_z+q\right)}\right] \tag{A9}$$

$$B_4=\cos\left(\phi_s-\phi\right)\left[\frac{\sin\theta\left(k_y+v\right)}{k_z+q}+\frac{\cos\theta\left(k_{sx}+u\right)\left(k_y+v\right)}{\left(k_{sz}-q\right)\left(k_z+q\right)}\right]$$

$$-\sin\left(\phi_s-\phi\right)\left[\cos\theta+\frac{\sin\theta\left(k_x+u\right)}{k_z+q}-\frac{\cos\theta\left(k_{sy}+v\right)\left(k_y+v\right)}{\left(k_{sz}-q\right)\left(k_z+q\right)}\right] \tag{A10}$$

$$B_5=-\cos\left(\phi_s-\phi\right)\left[\frac{v\left(k_{sx}+u\right)}{k_{sz}-q}+\frac{v\left(k_x+u\right)}{k_z+q}\right]+\sin\left(\phi_s-\phi\right)\left[q-\frac{v\left(k_{sy}+v\right)}{k_{sz}-q}-\frac{u\left(k_x+u\right)}{k_z+q}\right] \tag{A11}$$

$$B_6=\cos\left(\phi_s-\phi\right)\left[\frac{q\left(k_{sx}+u\right)\left(k_y+v\right)}{\left(k_{sz}-q\right)\left(k_z+q\right)}+\frac{u\left(k_y+v\right)}{k_z+q}\right]+\sin\left(\phi_s-\phi\right)\left[\frac{q\left(k_{sy}+v\right)\left(k_y+v\right)}{\left(k_{sz}-q\right)\left(k_z+q\right)}+\frac{v\left(k_y+v\right)}{k_z+q}\right] \tag{A12}$$

APPENDIX B.

In this appendix, we give coefficients appearing in Equation (28c).

$$a=k_i\left(\cos\theta_s+\cos\theta_i\right)\left|f_{qp}\right|^2 \tag{B1}$$

$$
\begin{aligned}
b = \frac{1}{2} &\left\{ f_{qp}^* \mathscr{F}_{qp}^+(-k_{ix},-k_{iy}) \left[k_i \cos\theta_s - k_{iz}\right]\left[k_i \cos\theta_s + k_i \cos\theta_i\right] \right. \\
&\left. + f_{qp}^* \mathscr{F}_{qp}^+(-k_{sx},-k_{sy})\left[k_i \cos\theta_s + k_{sz}\right]\left[k_i \cos\theta_s + k_i \cos\theta_i\right] \right\} \\
+ \frac{1}{2} &\left\{ f_{qp}^* \mathscr{F}_{qp}^-(-k_{ix},-k_{iy}) \left[k_i \cos\theta_s + k_{iz}\right]\left[k_i \cos\theta_s + k_i \cos\theta_i\right] \right. \\
&\left. + f_{qp}^* \mathscr{F}_{qp}^-(-k_{sx},-k_{sy})\left[k_i \cos\theta_s - k_{sz}\right]\left[k_i \cos\theta_s + k_i \cos\theta_i\right] \right\} \\
+ \frac{1}{2} &\left\{ f_{qp}^* \mathscr{G}_{qp}^+(-k_{ix},-k_{iy}) \left[k_i \cos\theta_s - \kappa_{tz}\right]\left[k_i \cos\theta_s + k_i \cos\theta_i\right] \right. \\
&\left. + f_{qp}^* \mathscr{G}_{qp}^+(-k_{sx},-k_{sy})\left[k_i \cos\theta_s + \kappa_{tsz}\right]\left[k_i \cos\theta_s + k_i \cos\theta_i\right] \right\} \\
+ \frac{1}{2} &\left\{ f_{qp}^* \mathscr{G}_{qp}^-(-k_{ix},-k_{iy}) \left[k_i \cos\theta_s + \kappa_{tz}\right]\left[k_i \cos\theta_s + k_i \cos\theta_i\right] \right. \\
&\left. + f_{qp}^* \mathscr{G}_{qp}^-(-k_{sx},-k_{sy})\left[k_i \cos\theta_s - \kappa_{tsz}\right]\left[k_i \cos\theta_s + k_i \cos\theta_i\right] \right\}
\end{aligned}
\tag{B2}
$$

$$
\begin{aligned}
c = \frac{1}{16} &\left\{ \mathscr{F}_{qp}^+(-k_{ix},-k_{iy})\,\mathscr{F}_{qp}^{+*}(-k_{ix},-k_{iy})\left[k_i \cos\theta_s - k_{iz}\right]\left[k_i \cos\theta_s - k_{iz}\right] \right. \\
&+ \mathscr{F}_{qp}^+(-k_{ix},-k_{iy})\,\mathscr{F}_{qp}^{+*}(-k_{sx},-k_{sy})\left[k_i \cos\theta_s - k_{iz}\right]\left[k_i \cos\theta_i + k_{sz}\right] \\
&+ \mathscr{F}_{qp}^+(-k_{sx},-k_{sy})\,\mathscr{F}_{qp}^{+*}(-k_{ix},-k_{iy})\left[k_i \cos\theta_i + k_{sz}\right]\left[k_i \cos\theta_s - k_{iz}\right] \\
&\left. + \mathscr{F}_{qp}^+(-k_{sx},-k_{sy})\,\mathscr{F}_{qp}^{+*}(-k_{sx},-k_{sy})\left[k_i \cos\theta_i + k_{sz}\right]\left[k_i \cos\theta_i + k_{sz}\right] \right\} \\
+ \frac{1}{16} &\left\{ \mathscr{F}_{qp}^+(-k_{ix},-k_{iy})\,\mathscr{F}_{qp}^{-*}(-k_{ix},-k_{iy})\left[k_i \cos\theta_s - k_{iz}\right]\left[k_i \cos\theta_s + k_{iz}\right] \right. \\
&+ \mathscr{F}_{qp}^+(-k_{ix},-k_{iy})\,\mathscr{F}_{qp}^{-*}(-k_{sx},-k_{sy})\left[k_i \cos\theta_s - k_{iz}\right]\left[k_i \cos\theta_i - k_{sz}\right] \\
&+ \mathscr{F}_{qp}^+(-k_{sx},-k_{sy})\,\mathscr{F}_{qp}^{-*}(-k_{ix},-k_{iy})\left[k_i \cos\theta_i + k_{sz}\right]\left[k_i \cos\theta_s + k_{iz}\right] \\
&\left. + \mathscr{F}_{qp}^+(-k_{sx},-k_{sy})\,\mathscr{F}_{qp}^{-*}(-k_{sx},-k_{sy})\left[k_i \cos\theta_i + k_{sz}\right]\left[k_i \cos\theta_i - k_{sz}\right] \right\} \\
+ \frac{1}{16} &\left\{ \mathscr{F}_{qp}^+(-k_{ix},-k_{iy})\,\mathscr{G}_{qp}^{+*}(-k_{ix},-k_{iy})\left[k_i \cos\theta_s - k_{iz}\right]\left[k_i \cos\theta_s - \kappa_{tz}\right] \right. \\
&+ \mathscr{F}_{qp}^+(-k_{ix},-k_{iy})\,\mathscr{G}_{qp}^{+*}(-k_{sx},-k_{sy})\left[k_i \cos\theta_s - k_{iz}\right]\left[k_i \cos\theta_i + \kappa_{tsz}\right] \\
&+ \mathscr{F}_{qp}^+(-k_{sx},-k_{sy})\,\mathscr{G}_{qp}^{+*}(-k_{ix},-k_{iy})\left[k_i \cos\theta_i + k_{sz}\right]\left[k_i \cos\theta_s - \kappa_{tz}\right] \\
&\left. + \mathscr{F}_{qp}^+(-k_{sx},-k_{sy})\,\mathscr{G}_{qp}^+ *(-k_{sx},-k_{sy})\left[k_i \cos\theta_i + k_{sz}\right]\left[k_i \cos\theta_i + \kappa_{tsz}\right] \right\} \\
+ \frac{1}{16} &\left\{ \mathscr{F}_{qp}^+(-k_{ix},-k_{iy})\,\mathscr{G}_{qp}^{-*}(-k_{ix},-k_{iy})\left[k_i \cos\theta_s - k_{iz}\right]\left[k_i \cos\theta_s + \kappa_{tz}\right] \right. \\
&+ \mathscr{F}_{qp}^+(-k_{ix},-k_{iy})\,\mathscr{G}_{qp}^{-*}(-k_{sx},-k_{sy})\left[k_i \cos\theta_s - k_{iz}\right]\left[k_i \cos\theta_i - \kappa_{tsz}\right] \\
&+ \mathscr{F}_{qp}^+(-k_{sx},-k_{sy})\,\mathscr{G}_{qp}^{-*}(-k_{ix},-k_{iy})\left[k_i \cos\theta_i + k_{sz}\right]\left[k_i \cos\theta_s + \kappa_{tz}\right] \\
&\left. + \mathscr{F}_{qp}^+(-k_{sx},-k_{sy})\,\mathscr{G}_{qp}^{-*}(-k_{sx},-k_{sy})\left[k_i \cos\theta_i + k_{sz}\right]\left[k_i \cos\theta_i - \kappa_{tsz}\right] \right\} \\
+ \frac{1}{16} &\left\{ \mathscr{F}_{qp}^-(-k_{ix},-k_{iy})\,\mathscr{F}_{qp}^{+*}(-k_{ix},-k_{iy})\left[k_i \cos\theta_s + k_{iz}\right]\left[k_i \cos\theta_s - k_{iz}\right] \right. \\
&+ \mathscr{F}_{qp}^-(-k_{ix},-k_{iy})\,\mathscr{F}_{qp}^{+*}(-k_{sx},-k_{sy})\left[k_i \cos\theta_s + k_{iz}\right]\left[k_i \cos\theta_i + k_{sz}\right] \\
&+ \mathscr{F}_{qp}^-(-k_{sx},-k_{sy})\,\mathscr{F}_{qp}^{+*}(-k_{ix},-k_{iy})\left[k_i \cos\theta_i - k_{sz}\right]\left[k_i \cos\theta_s - k_{iz}\right] \\
&\left. + \mathscr{F}_{qp}^-(-k_{sx},-k_{sy})\,\mathscr{F}_{qp}^{+*}(-k_{sx},-k_{sy})\left[k_i \cos\theta_i - k_{sz}\right]\left[k_i \cos\theta_i + k_{sz}\right] \right\} \\
+ \frac{1}{16} &\left\{ \mathscr{F}_{qp}^-(-k_{ix},-k_{iy})\,\mathscr{F}_{qp}^{-*}(-k_{ix},-k_{iy})\left[k_i \cos\theta_s + k_{iz}\right]\left[k_i \cos\theta_s + k_{iz}\right] \right. \\
&+ \mathscr{F}_{qp}^-(-k_{ix},-k_{iy})\,\mathscr{F}_{qp}^{-*}(-k_{sx},-k_{sy})\left[k_i \cos\theta_s + k_{iz}\right]\left[k_i \cos\theta_i - k_{sz}\right] \\
&+ \mathscr{F}_{qp}^-(-k_{sx},-k_{sy})\,\mathscr{F}_{qp}^{-*}(-k_{ix},-k_{iy})\left[k_i \cos\theta_i - k_{sz}\right]\left[k_i \cos\theta_s + k_{iz}\right] \\
&\left. + \mathscr{F}_{qp}^-(-k_{sx},-k_{sy})\,\mathscr{F}_{qp}^{-*}(-k_{sx},-k_{sy})\left[k_i \cos\theta_i - k_{sz}\right]\left[k_i \cos\theta_i - k_{sz}\right] \right\}
\end{aligned}
$$

$$+\frac{1}{16}\left\{\mathscr{F}_{qp}^{-}\left(-k_{ix},-k_{iy}\right)\mathscr{G}_{qp}^{+*}\left(-k_{ix},-k_{iy}\right)\left[k_{i}\cos\theta_{s}+k_{iz}\right]\left[k_{i}\cos\theta_{s}-k_{tz}\right]\right.$$

$$+\mathscr{F}_{qp}^{-}\left(-k_{ix},-k_{iy}\right)\mathscr{G}_{qp}^{+*}\left(-k_{sx},-k_{sy}\right)\left[k_{i}\cos\theta_{s}+k_{iz}\right]\left[k_{i}\cos\theta_{i}+k_{tsz}\right]$$

$$+\mathscr{F}_{qp}^{-}\left(-k_{sx},-k_{sy}\right)\mathscr{G}_{qp}^{+*}\left(-k_{ix},-k_{iy}\right)\left[k_{i}\cos\theta_{i}-k_{sz}\right]\left[k_{i}\cos\theta_{s}-k_{tz}\right]$$

$$+\left.\mathscr{F}_{qp}^{-}\left(-k_{sx},-k_{sy}\right)\mathscr{G}_{qp}^{+*}\left(-k_{sx},-k_{sy}\right)\left[k_{i}\cos\theta_{i}-k_{sz}\right]\left[k_{i}\cos\theta_{i}+k_{tsz}\right]\right\}$$

$$+\frac{1}{16}\left\{\mathscr{F}_{qp}^{-}\left(-k_{ix},-k_{iy}\right)\mathscr{G}_{qp}^{-*}\left(-k_{ix},-k_{iy}\right)\left[k_{i}\cos\theta_{s}+k_{iz}\right]\left[k_{i}\cos\theta_{s}+k_{tz}\right]\right.$$

$$+\mathscr{F}_{qp}^{-}\left(-k_{ix},-k_{iy}\right)\mathscr{G}_{qp}^{-*}\left(-k_{sx},-k_{sy}\right)\left[k_{i}\cos\theta_{s}+k_{iz}\right]\left[k_{i}\cos\theta-k_{tsz}\right]$$

$$+\left(\mathscr{F}_{qp}^{-}\left(-k_{sx},-k_{sy}\right)\mathscr{G}_{qp}^{-*}\left(-k_{ix},-k_{iy}\right)\left[k_{i}\cos\theta_{i}-k_{sz}\right]\left[k_{i}\cos\theta_{s}+k_{tz}\right]\right)$$

$$+\left.\mathscr{F}_{qp}^{-}\left(-k_{sx},-k_{sy}\right)\mathscr{G}_{qp}^{-*}\left(-k_{sx},-k_{sy}\right)\left[k_{i}\cos\theta_{i}-k_{sz}\right]\left[k_{i}\cos\theta_{i}-k_{tsz}\right]\right\}$$

$$+\frac{1}{16}\left\{\mathscr{G}_{qp}^{+}\left(-k_{ix},-k_{iy}\right)\mathscr{F}_{qp}^{+*}\left(-k_{ix},-k_{iy}\right)\left[k_{i}\cos\theta_{s}-\kappa_{tz}\right]\left[k_{i}\cos\theta_{s}-k_{iz}\right]\right.$$

$$+\mathscr{G}_{qp}^{+}\left(-k_{ix},-k_{iy}\right)\mathscr{F}_{qp}^{+*}\left(-k_{sx},-k_{sy}\right)\left[k_{i}\cos\theta_{s}-\kappa_{tz}\right]\left[k_{i}\cos\theta_{i}+k_{sz}\right]$$

$$+\mathscr{G}_{qp}^{+}\left(-k_{sx},-k_{sy}\right)\mathscr{F}_{qp}^{+*}\left(-k_{ix},-k_{iy}\right)\left[k_{i}\cos\theta_{i}+\kappa_{tsz}\right]\left[k_{i}\cos\theta_{s}-k_{iz}\right]$$

$$+\left.\mathscr{G}_{qp}^{+}\left(-k_{sx},-k_{sy}\right)\mathscr{F}_{qp}^{+*}\left(-k_{sx},-k_{sy}\right)\left[k_{i}\cos\theta_{i}+\kappa_{tsz}\right]\left[k_{i}\cos\theta_{i}+k_{sz}\right]\right\}$$

$$+\frac{1}{16}\left\{\mathscr{G}_{qp}^{+}\left(-k_{ix},-k_{iy}\right)\mathscr{F}_{qp}^{-*}\left(-k_{ix},-k_{iy}\right)\left[k_{i}\cos\theta_{s}-\kappa_{tz}\right]\left[k_{i}\cos\theta_{s}+k_{iz}\right]\right.$$

$$+\mathscr{G}_{qp}^{+}\left(-k_{ix},-k_{iy}\right)\mathscr{F}_{qp}^{-*}\left(-k_{sx},-k_{sy}\right)\left[k_{i}\cos\theta_{s}-\kappa_{tz}\right]\left[k_{i}\cos\theta_{i}-k_{sz}\right]$$

$$+\mathscr{G}_{qp}^{+}\left(-k_{sx},-k_{sy}\right)\mathscr{F}_{qp}^{-*}\left(-k_{ix},-k_{iy}\right)\left[k_{i}\cos\theta_{i}+\kappa_{tsz}\right]\left[k_{i}\cos\theta_{s}+k_{iz}\right]$$

$$+\left.\mathscr{G}_{qp}^{+}\left(-k_{sx},-k_{sy}\right)\mathscr{G}_{qp}^{-*}\left(-k_{sx},-k_{sy}\right)\left[k_{i}\cos\theta_{i}+\kappa_{tsz}\right]\left[k_{i}\cos\theta_{i}-k_{sz}\right]\right\}$$

$$+\frac{1}{16}\left\{\mathscr{G}_{qp}^{+}\left(-k_{ix},-k_{iy}\right)\mathscr{G}_{qp}^{+*}\left(-k_{ix},-k_{iy}\right)\left[k_{i}\cos\theta_{s}-\kappa_{tz}\right]\left[k_{i}\cos\theta_{s}-k_{tz}\right]\right.$$

$$+\mathscr{G}_{qp}^{+}\left(-k_{ix},-k_{iy}\right)\mathscr{G}_{qp}^{+*}\left(-k_{sx},-k_{sy}\right)\left[k_{i}\cos\theta_{s}-\kappa_{tz}\right]\left[k_{i}\cos\theta_{i}+k_{tsz}\right]$$

$$+\mathscr{G}_{qp}^{+}\left(-k_{sx},-k_{sy}\right)\mathscr{G}_{qp}^{+*}\left(-k_{ix},-k_{iy}\right)\left[k_{i}\cos\theta_{i}+\kappa_{tsz}\right]\left[k_{i}\cos\theta_{s}-k_{tz}\right]$$

$$+\left.\mathscr{G}_{qp}^{+}\left(-k_{sx},-k_{sy}\right)\mathscr{G}_{qp}^{+*}\left(-k_{sx},-k_{sy}\right)\left[k_{i}\cos\theta_{i}+\kappa_{tsz}\right]\left[k_{i}\cos\theta_{i}+k_{tsz}\right]\right\}$$

$$+\frac{1}{16}\left\{\mathscr{G}_{qp}^{+}\left(-k_{ix},-k_{iy}\right)\mathscr{G}_{qp}^{-*}\left(-k_{ix},-k_{iy}\right)\left[k_{i}\cos\theta_{s}-\kappa_{tz}\right]\left[k_{i}\cos\theta_{s}+k_{tz}\right]\right.$$

$$+\mathscr{G}_{qp}^{+}\left(-k_{ix},-k_{iy}\right)\mathscr{G}_{qp}^{-*}\left(-k_{sx},-k_{sy}\right)\left[k_{i}\cos\theta_{s}-\kappa_{tz}\right]\left[k_{i}\cos\theta_{i}-k_{tsz}\right]$$

$$+\mathscr{G}_{qp}^{+}\left(-k_{sx},-k_{sy}\right)\mathscr{G}_{qp}^{-*}\left(-k_{ix},-k_{iy}\right)\left[k_{i}\cos\theta_{i}+\kappa_{tsz}\right]\left[k_{i}\cos\theta_{s}+k_{tz}\right]$$

$$+\left.\mathscr{G}_{qp}^{+}\left(-k_{sx},-k_{sy}\right)\mathscr{G}_{qp}^{-*}\left(-k_{sx},-k_{sy}\right)\left[k_{i}\cos\theta_{i}+\kappa_{tsz}\right]\left[k_{i}\cos\theta_{i}-k_{tsz}\right]\right\} \tag{B3}$$

where $k_{tsz}=\sqrt{k_{t}^{2}-k_{sx}^{2}-k_{sy}^{2}}$.

REFERENCES

1. Beckman, P. and A. Spizzichino, *The Scattering of Electromagnetic Waves from Rough Surfaces*, Pergamon Press, Oxford, 1963.
2. Ulaby, F. T., R. K. Moore, and A. K. Fung, *Microwave Remote Sensing*, Vol. 2, Chapter 12, Artech House, Norwood, MA, 1982.
3. Fung, A. K., *Microwave Scattering and Emission Models and Their Applications*, Artech House, Norwood, MA, 1994.
4. Voronovich, A. G., *Wave Scattering from Rough Surfaces*, Springer-Verlag, Berlin, 1994.
5. Tsang, L. and J. A. Kong, *Scattering of Electromagnetic Waves: Advanced Topics*, Chapters 1, 2, John Wiley & Sons, 2001.

6. Fung, A. K. and K. S. Chen, *Microwave Scattering and Emission Models for Users*, Artech House, Norwood, MA, 2009.

7. Fung, A. K., Q. Li, and K. S. Chen, "Backscattering from a randomly rough dielectric surface," *IEEE Trans. Geoscience and Remote Sensing*, Vol. 30, No. 2, 356–369, 1992.

8. Chen, K. S., A. K. Fung, and D. E. Weissman, "A backscattering model for sea surfaces," *IEEE Trans. Geoscience and Remote Sensing*, Vol. 30, No. 4, 811–817, 1992.

9. Hsieh, C. Y., A. K. Fung, G. Nesti, G. A. Sieber, and P. Coppo, "A further study of the IEM surface scattering model," *IEEE Trans. Geoscience and Remote Sensing* , Vol. 35, 901–909, 1997.

10. Chen, K. S., T.-D. Wu, M.-K. Tsay, and A. K. Fung, "A note on the multiple scattering in an IEM model," *IEEE Trans. Geoscience and Remote Sensing*, Vol. 38, No. 1, 249–256, 2000.

11. Wu, T. D., K. S. Chen, J. C. Shi, and A. K. Fung, "A transition model for the reflection coefficient in surface scattering," *IEEE Trans. Geoscience and Remote Sensing*, Vol. 39, No. 9, 2040–2050, 2001.

12. Álvarez-Pérez, J., "An extension of the IEM/IEMM surface scattering model," *Waves in Random Media*, Vol. 11, No. 3, 307–329, 2001.

13. Fung, A. K., W. Y. Liu, K. S. Chen, and M. K. Tsay, "An improved IEM model for bistatic scattering," *Journal of Electromagnetic Waves and Applications*, Vol. 16, No. 5, 689–702, 2002.

14. Chen, K. S., T.-D. Wu, L. Tsang, Q. Li, J. C. Shi, and A. K. Fung, "Emission of rough surfaces calculated by the integral equation method with comparison to three-dimensional moment method simulations," *IEEE Trans. Geoscience and Remote Sensing*, Vol. 41, No. 1, 90–101, 2003.

15. Wu, T. D. and K. S. Chen, "A reappraisal of the validity of the IEM model for backscattering from rough surfaces," *IEEE Trans. Geoscience and Remote Sensing*, Vol. 42, No. 8, 743–753, 2004.

16. Fung, A. K. and K. S. Chen, "An update on IEM surface backscattering model," *IEEE Geoscience and Remote Sensing Letters*, Vol. 1, No. 2, 75–77, 2004.

17. Du, Y., "A new bistatic model for electromagnetic scattering from randomly rough surfaces," *Waves Random Complex Media*, Vol. 18, No. 1, 109–128, 2008.

18. Wu, T. D., K. S. Chen, J. C. Shi, H. W. Lee, and A. K. Fung, "A study of AIEM model for bistatic scattering from randomly surfaces," *IEEE Trans. Geoscience and Remote Sensing*, Vol. 46, No. 9, 2584–2598, 2008.

19. Álvarez-Pérez, J. L., "The IEM2M rough-surface scattering model for complex-permittivity scattering media," *Waves Random Complex Media*, Vol. 22, No. 2, 207–233, 2012.

20. Poggio, A. J. and E. K. Miller, "Integral equation solution of three dimensional scattering problems," *Computer Techniques for Electromagnetics*, R. Mittra (ed.), Pergamon, New York, 1973.

21. Li, Z. and A. K. Fung, "A reformulation of the surface field integral equation," *Journal of Electromagnetic Waves and Application*, Vol. 5, No. 2, 195–203, 1991.

22. Li, Q., J. C. Shi, and K. S. Chen "A generalized power law spectrum and its applications to the backscattering of soil surfaces based on the integral equation model," *IEEE Trans. Geoscience and Remote Sensing*, Vol. 40, No. 2, 271–281, 2002.

23. Ewe, H. T., J. T. Johnson, and K. S. Chen, "A comparison study of the surface scattering models and numerical model," *Proceedings of IGARSS' 01*, Vol. 6, 2692–2694, 2001.